nature neuroscience

Supplementary information

https://doi.org/10.1038/s41593-025-02064-4

Brain tumors induce widespread disruption of calvarial bone and alteration of skull marrow immune landscape

In the format provided by the authors and unedited

Supplementary Fig. 1

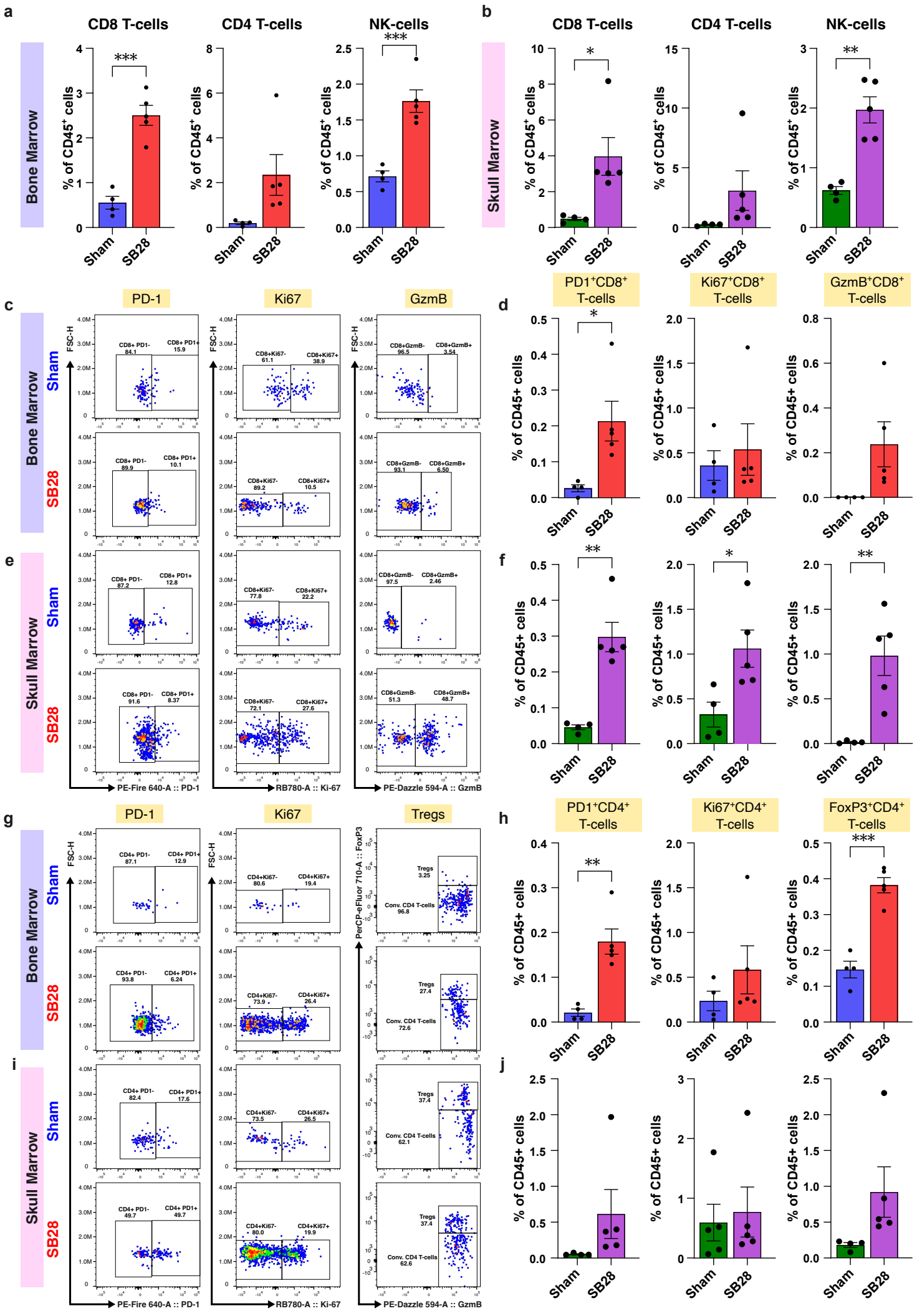

Supplementary Fig. 1. Flow cytometry analysis showing functional characteristics of main lymphoid population (CD4, CD8, NK cells) in SM and BM of SB28 tumor bearing mice (a-b)**.**

(c-e) FACS dot plots showing CD8 expressing PD1, KI67 or GzmB out of CD45+ cells in BM and SM.

(d-f) quantification of CD8 expressing PD1, KI67, GzmB showing significant difference in SM, while only PD1 was significant in BM.

(c-e) FACS dot plots showing CD4 expressing PD1, KI67 or FoxP3 out of CD45+ cells in BM and SM.

(h-j) Quantification of CD4 expressing PD1, KI67 or FoxP3 out of CD45+ cells in BM and SM. PD1 and FoxP3 were significantly higher in BM of tumor bearing animals compared to sham,

Number of animals in statistics: in (a, b, d, f, h, j), 4 mice/sham; 5 mice/SB28. Data are presented as means ± SEM. Significance was assessed as Mann-Whitney U test (*, $p < 0.05$; **, $p < 0.01$; *** $p < 0.001$).

Supplementary Fig. 2

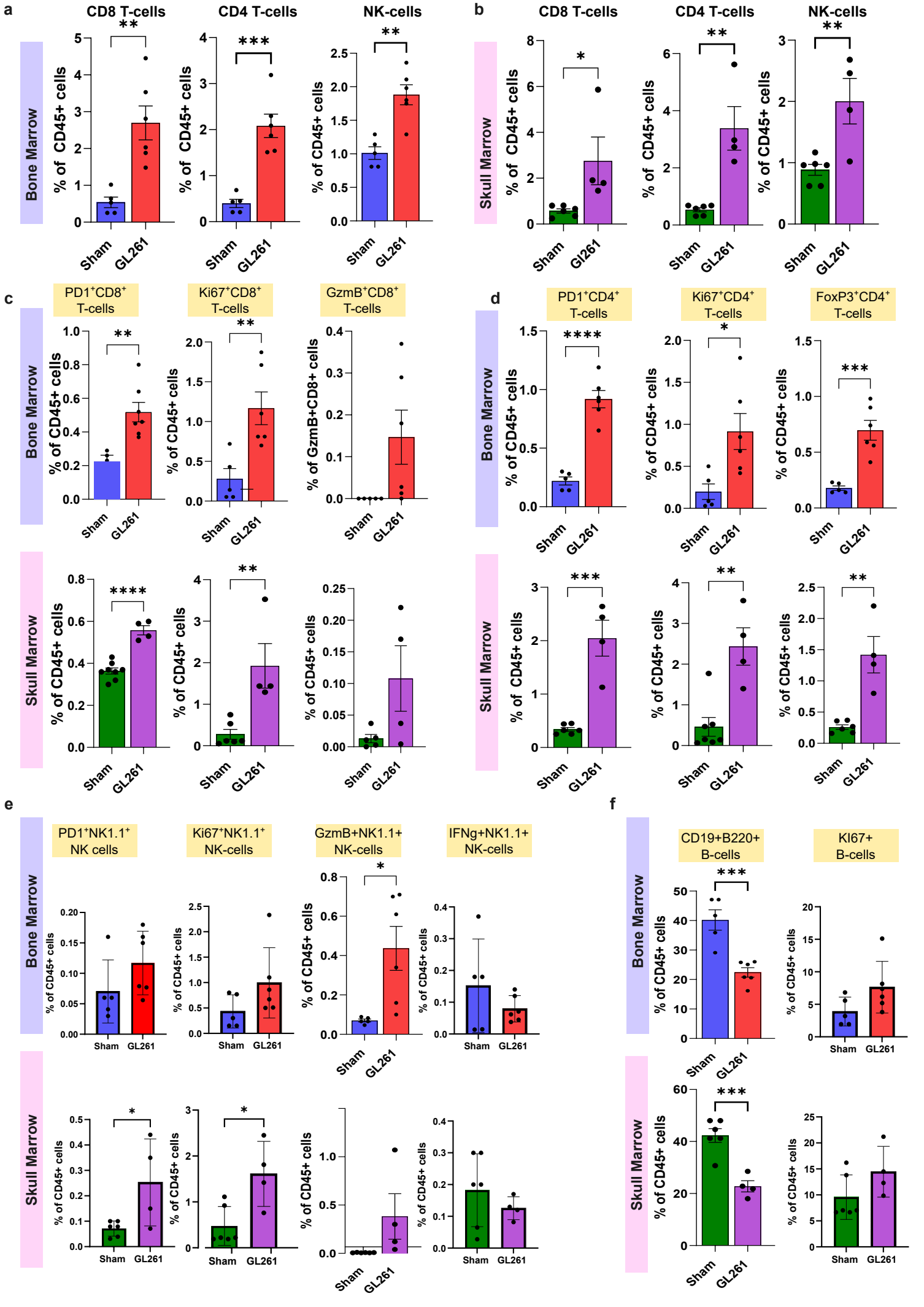

Supplementary Fig. 2. Flow cytometry analysis showing functional characteristics of main population (CD4, CD8, NK cells) in SM and BM of GL261 tumor bearing mice (a-b)**.**

(c) Frequency of CD8 expressing PD1, KI67 or GzmB out of CD45+ cells in BM and SM. Both PD1 and KI67 were significantly higher in tumor BM and SM compared to sham.
(d) Frequency of CD4 expressing PD1, KI67 or FoxP3 out of CD45+ cells in BM and SM. All 3 markers were significantly higher in BM and SM from tumor bearing animals compared to sham,
(e) Frequency of NK cells expressing PD1, KI67 or GzmB, IFNg out of CD45+ cells in BM and SM. PD1 and KI67 were higher in SM NK compared to sham, but GzmB was higher in BM vs sham.
(f) Frequency of B cells and KI67 out of total CD45+ in BM and SM

Number of animals in statistics: in (a), 5 mice/sham; 6 mice/GL261; in (b), 6 mice/sham; 4 mice/GL261; in (c), Bone marrow (3 mice/sham; 7 mice/GL261), Skull marrow (8 mice/sham; 4 mice/GL261); in (d), Bone marrow (5 mice/sham; 6 mice/GL261), Skull marrow (6 mice/sham; 5 mice/GL261); in (e-f), Bone marrow (5 mice/sham; 6 mice/GL261), Skull marrow (6 mice/sham; 4 mice/GL261). Data are presented as means ± SEM. Significance was assessed as Mann-Whitney U test (*, $p < 0.05$; **, $p < 0.01$; *** $p < 0.001$; ****, $p < 0.0001$).

Supplementary Fig. 3

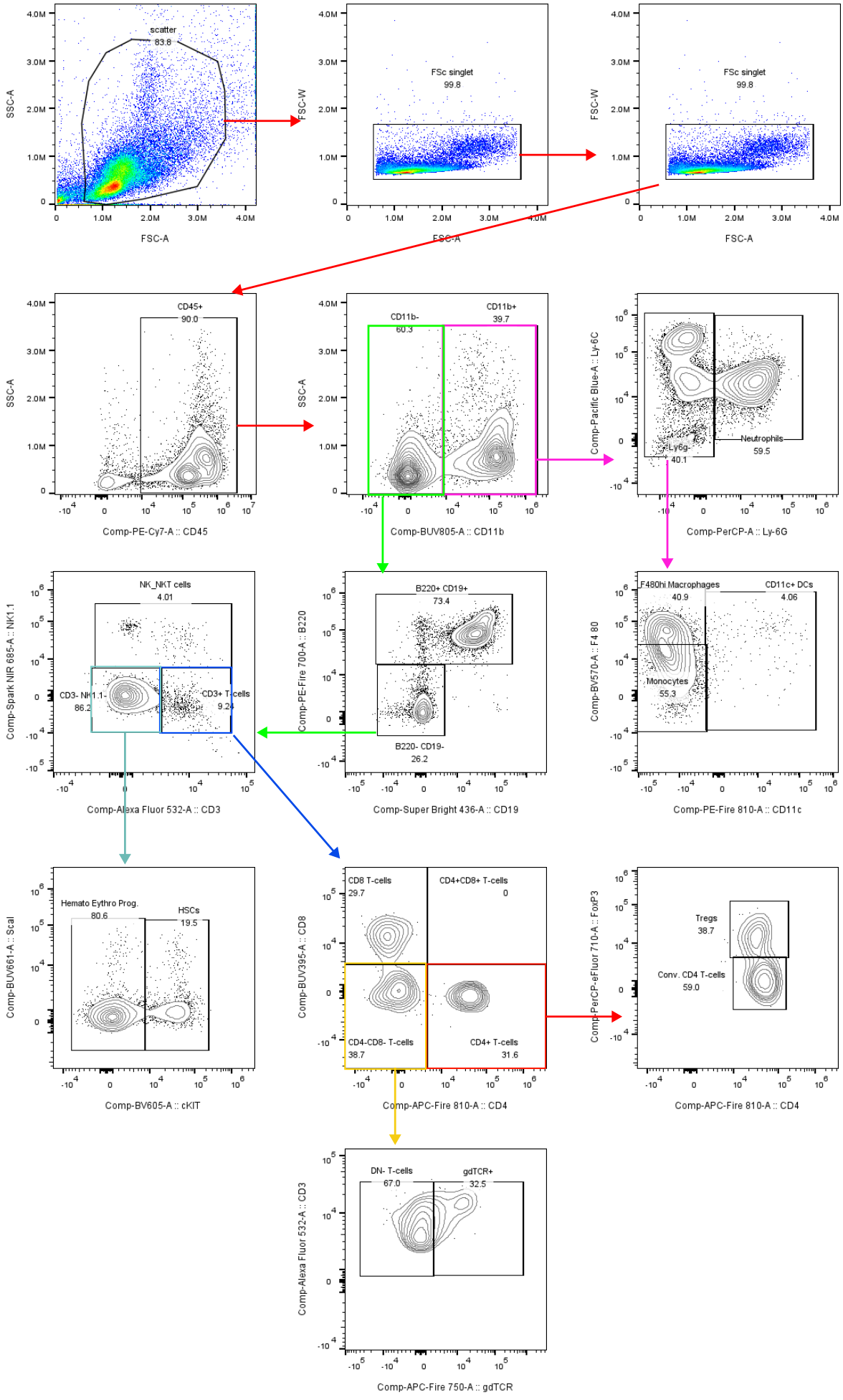

Supplementary Fig.3 Flow cytometry gating strategy of main immune cells population in SM and BM.

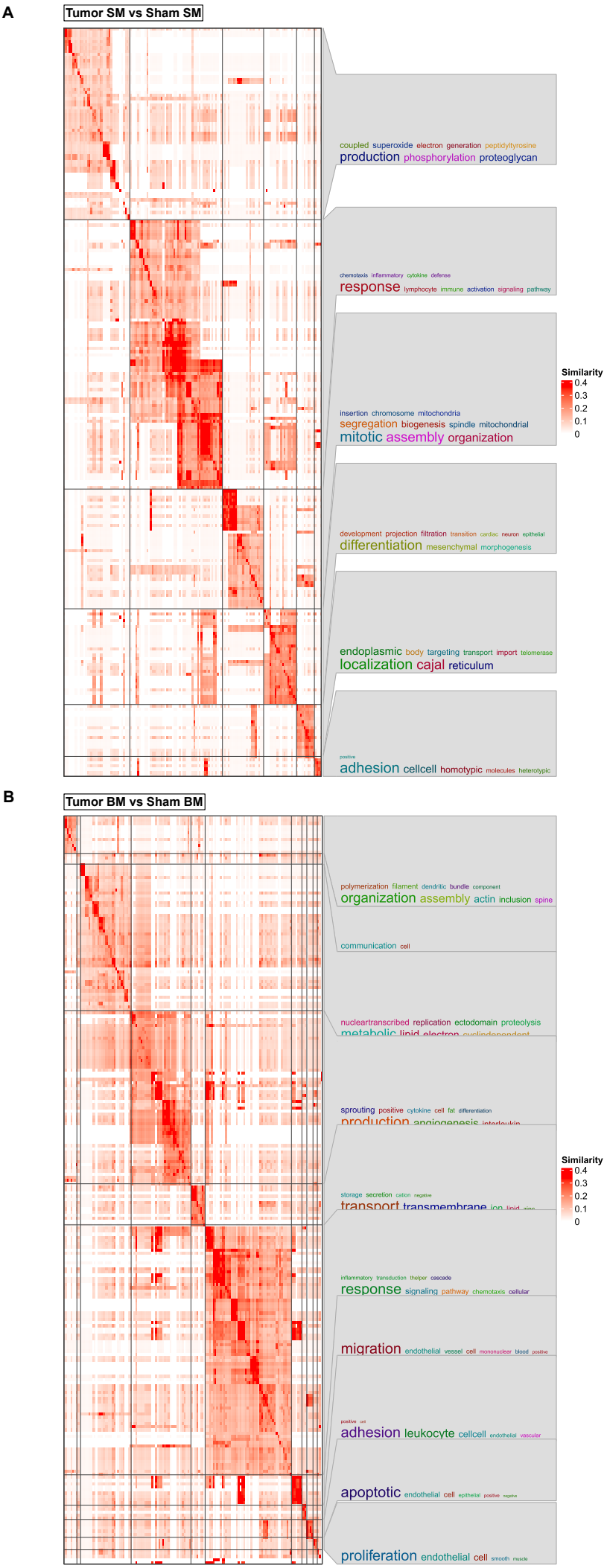

Supplementary Fig. 4. Semantic Clustering of GO terms enriched in response to tumor in SM and BM across myeloid lineages. Heatmaps depicting clustering of enriched GO terms in response to both GL261 and SB28 across different myeloid lineage cell types in either SM (A) or BM (B).

Supplementary Fig. 5

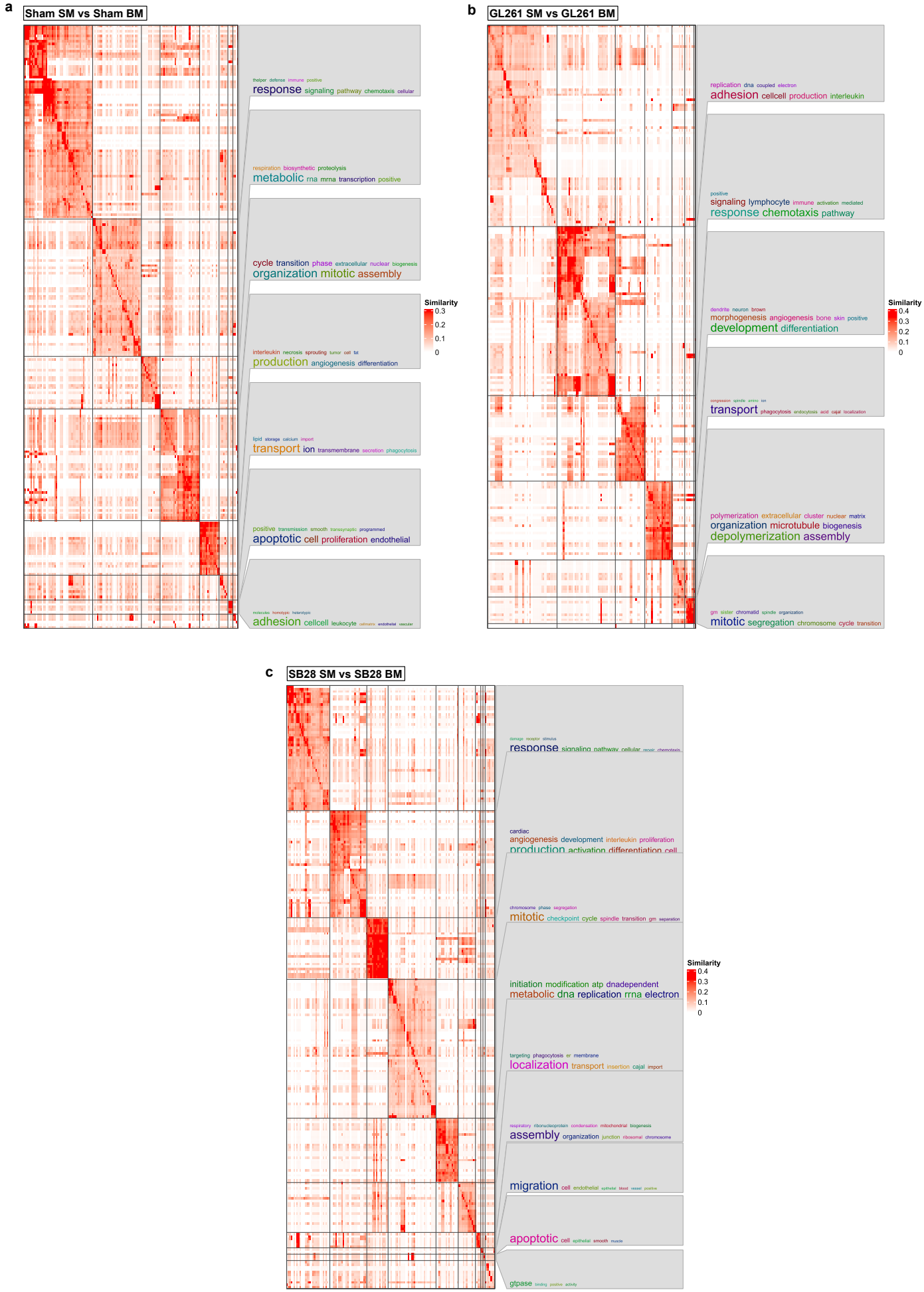

Supplementary Fig. 5. Semantic Clustering of GO terms enriched in SM vs BM comparisons across myeloid lineages. Heatmaps depicting clustering of enriched GO terms in SM vs BM analysis in Sham (A), GL261 (B) or SB28 (C) across all myeloid lineage cell types

Supplementary Fig. 6

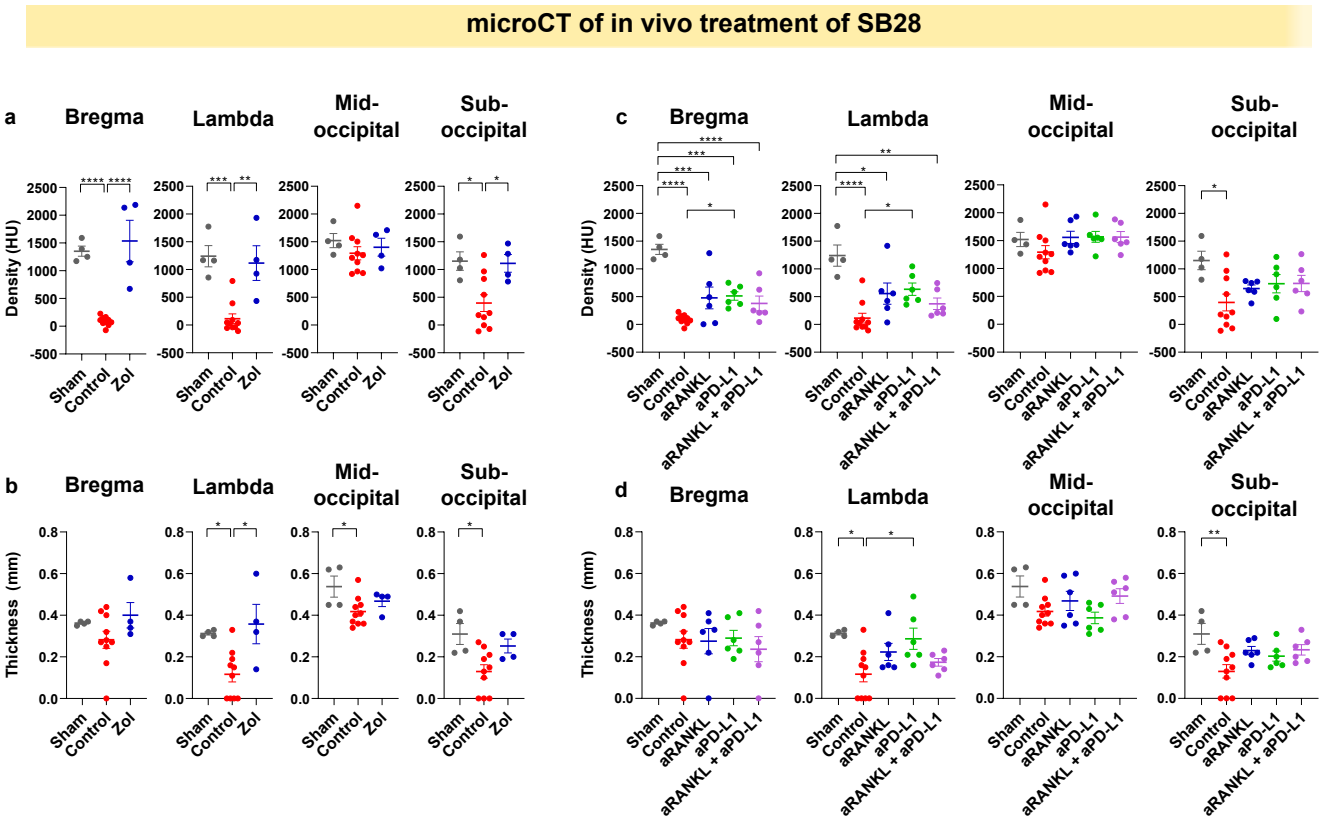

Supplementary Fig. 6 (Belong to Fig. 8). Zol treatment is effective in inhibiting bone resorption.
(a) Statistics analysis of bone density (b) and thickness showed that Zol treatment inhibited bone resorption.
(c) and (d) Statistics analysis of bone density and thickness microCT imaging showed that aRANKL didn't inhibit osteoclast activity at edges of fused skull bones. Number of mice per group in microCT: 4/sham, 4/zol, 10/control, 6/aRANKL, 6/aPD-L1, 6/aPD-L1+aRANKL. Data are presented means ± SEM. Significance was assessed a one-way ANOVA with Tukey's multiple comparison test (*, $p < 0.05$; **, $p < 0.01$; *** $p < 0.001$; ****, $p < 0.0001$). See also Figure S16.

in microCT: 4/sham, 4/zol, 10/control, 6/aRANKL, 6/aPD-L1, 6/aPD-L1+aRANKL. Data are presented means ± SEM (p values represent a one-way ANOVA with Tukey 'multiple comparison test).
See also Figure S16

Supplementary Fig. 7

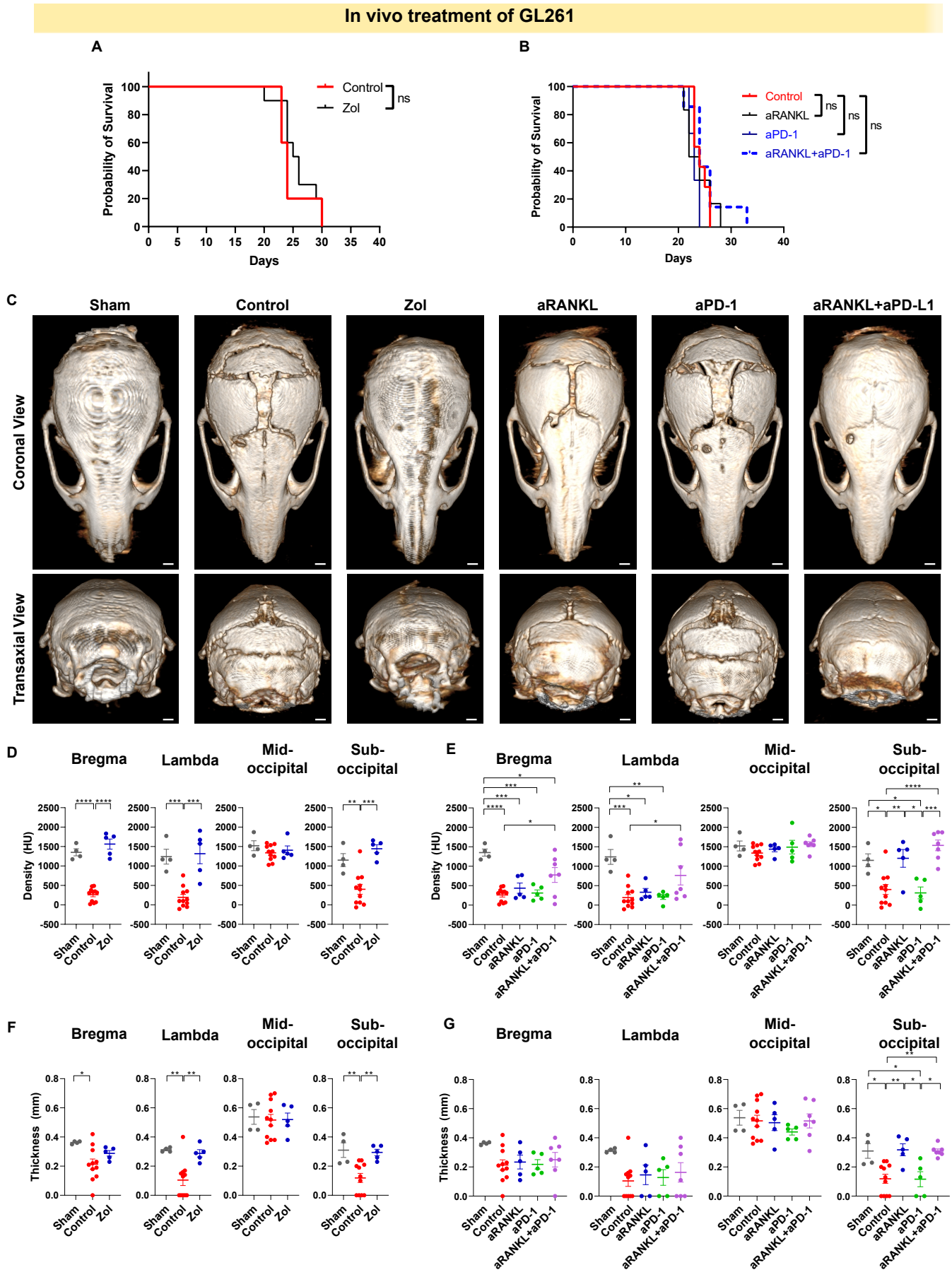

Supplementary Fig. 7 (Related to Figure 8). **In vivo treatment of GL261 showing no survival benefit of inhibiting Osteoclast activity.**

(A) KM survival in GL261 tumor- bearing mice, treatment started day10 with 3mg/kg s.c of Zol 3 times a week, treatment lasted 2 weeks. Zol treatment did not affect tumor progression (9 mice/Zol group, 5/control).

(B) Both, aPD-L1 (i.p 200ug/mouse) and aRANKL antibody (s.c 5mg/kg) did not have survival benefit as single treatment or combination in GL261 brain tumors (7/control, 6/aPD-1, 6/aRANKL, 7/aPD-1+aRANKL), P value 0.23 calculated using Log-rank (Mantel-Cox) test.

(C) Coronal and transaxial view of microCT imaging showing the efficacy of Zol in inhibiting skull bone resorption in last stage GL261 tumor bearing mice, aRANKL did not stop bone resorption, neither combination did.

(D-E) Zol treatment in GL261 inhibited bone resorption is shown with statistics analysis of bone density and thickness of microCT images. number of mice per group: 4/sham, 5/zol, 11/control,

(F-G) aRANKL alone or in combination with aPD1 treatment is shown with statistics analysis of bone density and thickness of microCT images 5/aRANKL, 5/aPD-1, 7/aPD-1+aRANKL. Data are presented means ± SEM (p values represent a one-way ANOVA with Tukey ‘multiple comparison test).

Supplementary Fig. 8

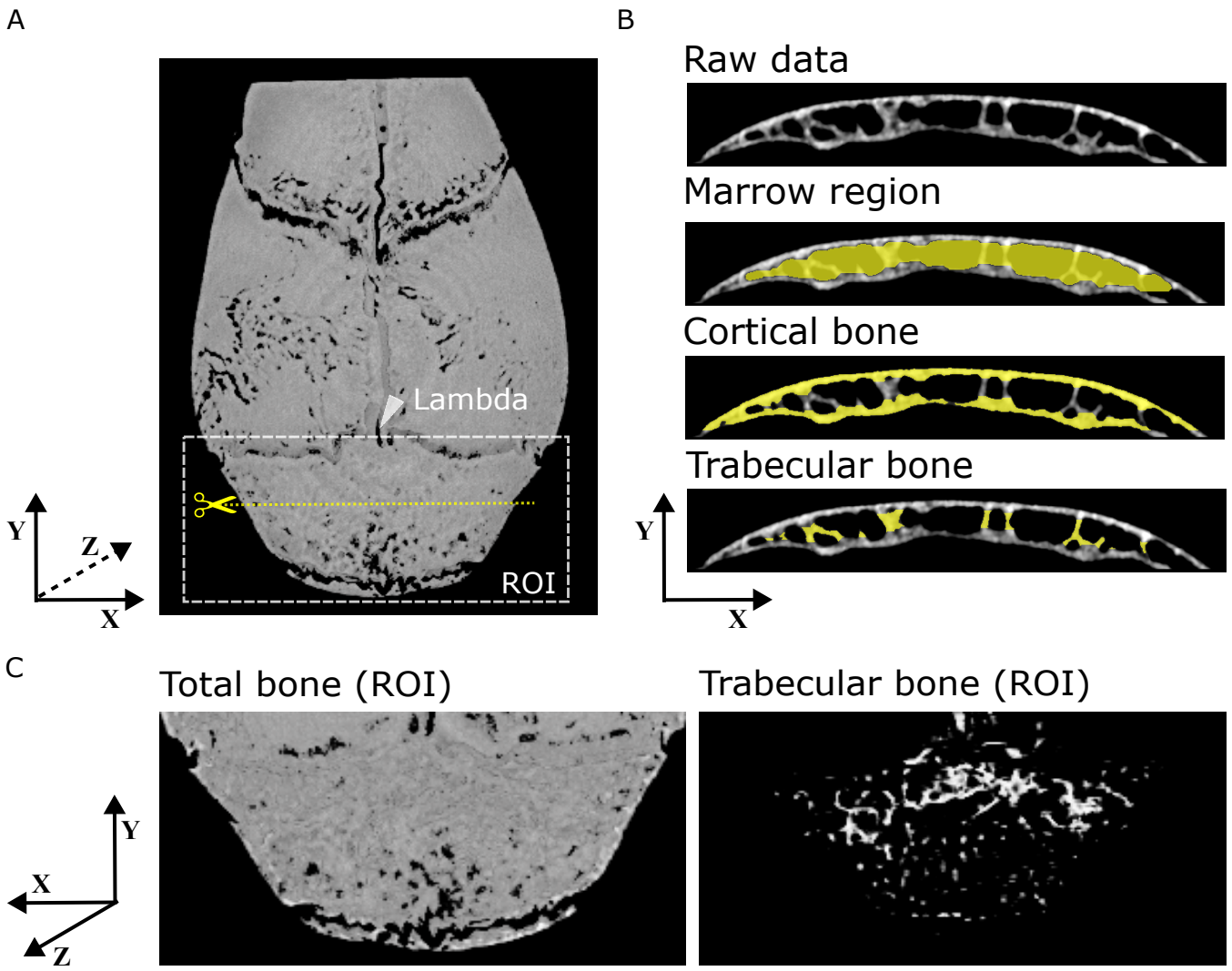

Supplementary Fig. 8. Example of the bone structure analysis on skull. (A) The region of interest (ROI), outlined by a white dotted line, was defined as the area posterior to Lambda in the reconstructed three-dimensional micro-CT image data.

(B) Slice view along the yellow dotted line in (A), illustrating each analysis step: Marrow region detection, Cortical bone detection, and trabecular bone detection.

(C) Three-dimensional representation of the total bone and trabecular bone within the ROI.

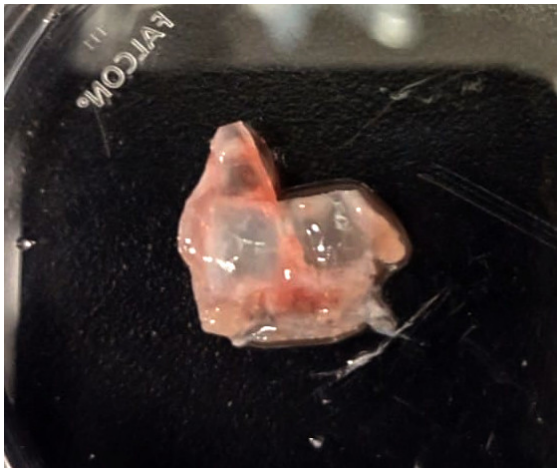

Supplementary Fig. 9. Representative image of the skull biopsy used for scRNA-seq experiment.